Assessment of smoothing and scale change effects on emergent aquatic vegetation in high spatial resolution image segmentation

Letícia Mayumi Matsuda ¹, Nilton Nobuhiro Imai ^{1,2}, Adilson Berveglieri ¹

¹ Graduate Program in Cartographic Sciences - PPGCC, São Paulo State University – UNESP, Presidente Prudente, São Paulo, Brazil - (leticia.matsuda, nilton.imai, a.berveglieri)@unesp.br
² Dept. of Cartography, São Paulo State University - UNESP, Presidente Prudente, São Paulo, Brazil

Keywords: Aquatic vegetation segmentation, High spatial resolution images, Smoothing, Subsampling.

Abstract

Identifying emergent aquatic vegetation (EAV) species is important to monitor environmental changes and support in decision-making. With the advent of uncrewed aerial vehicle (UAV), it has been possible to acquire high resolution images and assist in this task. At the same time, the high level of detail of these images can be considered noise for some segmentation algorithms and testing different smoothing and subsampling variations can be very relevant. Hence, the aim of this study is to analyse the performance of three segmentation algorithms (region growing, SLIC superpixel and watershed) to generate "homogeneous" regions in high resolution images, considering blur and scale change effects. To do this, images of a lake impacted by EAV were captured using a multispectral camera on board of UAV with 8 mm ground sample distance. After image processing, an orthomosaic was produced and three clippings were extracted from it to be segmented and tested empirically with variations of subsampling (1 cm, 1.6 cm, 2 cm, and 3 cm) and standard deviation smooth filter application ($\sigma = 2$, 4, and 8). The results showed that region growing and watershed algorithms are the most affected by high spatial resolution, and greatly benefits from the smoothing and subsampling applied, i.e., reducing the amount of detail, while superpixel algorithm created more consistent and uniform results, especially after smoothing, as evidenced by the quantitative evaluation based on segment entropy, characterized by kurtosis.

1. Introduction

Image segmentation is a fundamental technique used to split an image into relatively homogeneous and meaningful regions (Blaschke, 2010; Hossain and Chen, 2019). These regions, which represent semantically significant groups of pixels, become objects of image analysis (Blaschke, 2010) and can correspond to various land cover types, such as vegetation, water bodies, urban infrastructures, agricultural area etc.

Object based image analysis (OBIA) appeared in the remote sensing scenario with the advent of high spatial resolution imagery. In these cases, the pixel size is often smaller than the object of interest, requiring a processing step to make the image content more interpretable (Blaschke et al., 2014). OBIA consists of two main steps: segmentation, which groups pixels into meaningful objects, and classification, which assigns these objects to specific categories (Hossain and Chen, 2019).

Many segmentation algorithms originate from computer vision applications, including region growing (Bins et al., 1996), superpixel-based methods (Achanta et al., 2012), and watershed segmentation (Inglada and Christophe, 2009; Kornilov and Safonov, 2018). These algorithms are commonly used in remote sensing applications, as pointed out by Hossain and Chen (2019).

Region growing is known for its simplicity, grouping pixels that are spatially close and have similar intensity values (Espindola et al., 2006). Superpixel methods, such as simple linear iterative clustering (SLIC), offer an efficient way to generate compact and boundary-adherent segments, making them popular due to their computational efficiency and accuracy (Achanta et al., 2012). The watershed algorithm, based on mathematical morphology, provides precise boundary adherence and is commonly used for image segmentation (Sun and He, 2008).

Different segmentation algorithms have been applied in aquatic vegetation studies for detection, mapping, classification, and monitoring. In this context, many recent studies have employed semantic segmentation, a deep learning-based approach, using satellite or uncrewed aerial vehicle (UAV) imagery (Liu et al., 2022; Alagialoglou et al., 2023; Yu et al., 2024). Specific research has also focused on submerged aquatic vegetation (SAV) (Brooks et al. 2022; Alagialoglou et al., 2023; Wang et al., 2023). However, fewer recent studies have explored segmentation techniques for emergent aquatic vegetation (EAV) using non-deep learning approaches. For example, Szabó et al. (2024) applied a region growing algorithm to map aquatic vegetation, including EAV. Older studies, such as Benjamin et al. (2021) and Zhou et al. (2021), employed multiresolution segmentation algorithm, while Bolch et al. (2021) used a largescale mean-shift algorithm, all aiming to identify and map different EAV types.

Both EAV and SAV are rooted to the substrate, EAV characterizes for being partially under water and remains growing above water's surface, SAV are completely under water (Ashworth, 2023). These plants are important in the dynamics and biodiversity of aquatic ecosystems. However, uncontrolled growth can have negative environmental consequences, as is the case with the invasive and rapidly expanding water hyacinth (*Eichhornia crassipes*), which threatens ecosystem services and multiple water resource uses (Singh et al., 2020; Mqingwana et al., 2024). With the advent of images acquired by UAV, identifying EAV species has become highly feasible and important for decision-making, management, and water resource protection.

High spatial resolution imagery provides a rich level of scene detail, but this can also introduce challenges for segmentation. Some algorithms may interpret fine details as noise, leading to over-segmentation, where too many small, fragmented segments are created. On the other hand, insufficient detail can result in

under-segmentation, where meaningful objects are not properly delineated. Thus, this study aims to analyse the performance of three segmentation algorithms (region growing, superpixel, and watershed) when applied to high resolution images containing EAV, using kurtosis of entropy values to assess a normal probability distribution, i.e., internal homogeneity of the segments. Moreover, the impact of scale variations and smoothing effects will be examined, as these pre-processing adjustments can enhance the results of different segmentation algorithms.

2. Materials and method

Multispectral images of a reservoir with EAV occurrence were acquired by a Sony Alpha 6000 camera model, with effective focal length 25 mm, 4 bands (450 nm: blue, 550 nm: green, 650 nm: red, and 850 nm: near-infrared) in a 2512 x 3976 pixels frame and pixel size 0.0039 mm. The camera was on board of a UAV, with a flight height of 50 m. As a result, an orthomosaic was obtained with a ground sample distance (GSD) of 8 mm and three clippings (images) were extracted from it, containing three species of EAV to be segmented: water hyacinth (*Eichhornia crassipes*), alligator weed (*Alternanthera philoxeroides*) and cattails (*Typha domingensis*).

The approach applied in the study consisted of obtaining three image clippings with EAV, which were analysed at four subsampling levels (scale change): 1 cm; 1.6 cm; 2 cm; and 3 cm. The bilinear interpolation was used due to its smoother visual aspect, without the geometric discontinuities of the nearestneighbour, and computationally faster than cubic convolution (Roy and Dikshit, 1994; Arif and Akbar, 2005). Additionally, the clippings were also smoothed by the Gaussian filter with standard deviation (σ = 2, 4 and 8), assumed its characteristic of not only reducing noise, but effectively blurring the image (Hossain and Chen, 2019). Both spatial resolution and standard deviation were defined empirically.

In the following step, three segmentation algorithms were tested on the three clippings: region growing, superpixel, and watershed. The region growing algorithm was performed in Spring 5.5.6 software (Bins et al., 1996) by defining parameters of similarity and area threshold. The superpixel algorithm was applied with Python scikit-image 0.18.3 library (Van Der Walt et al., 2014), which only requires setting the k parameter. Finally, the Watershed algorithm was applied using the QGIS 3.20.3-Odense software, integrated with the Orfeo ToolBox 7.3.0 library (Inglada and Christophe, 2009). The depth threshold and flood level parameters were defined to control the segmentation process.

The quality of segmentation was evaluated with the calculation of entropy for all the segments throughout bands (4) and clippings (3), summarized by kurtosis. In this context, entropy represents the degree of complexity or heterogeneity within segments (Long and Singh, 2013) and was calculated with Python scikit-image 0.25.2 library (Van Der Walt et al., 2014). In statistical terms, kurtosis measures the shape of the tails of a probability distribution (Hyvärinen and Oja, 2000; Du and Kopriva, 2008). It can be either positive (leptokurtic) or negative (platykurtic), while a normal distribution (Gaussian) has zero kurtosis. This metric was computed with Python scipy 1.15.3 (Virtanen et al., 2020).

3. Experiments and results

The experiments are organized and presented by algorithm. To better illustrate the clippings, Figure 1 shows clipping 1 (Figure 1a) that incorporate water hyacinth and alligator weed; Clipping 2 (Figure 1b) includes water hyacinth and cattails; and Clipping 3 (Figure 1c) features alligator weed and cattails. Thus, each clipping consists of two EAV species to be separated.

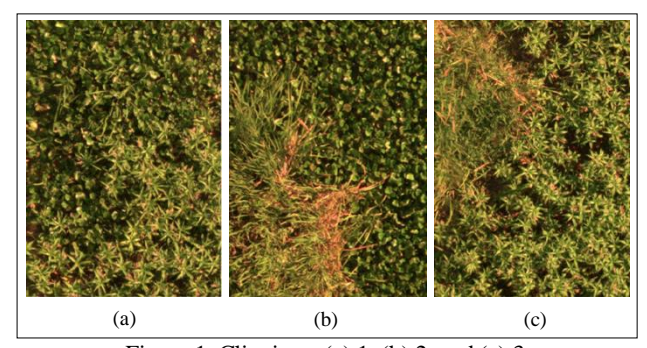


Figure 1. Clippings: (a) 1, (b) 2, and (c) 3.

3.1 Experiment 1: Region growing

The region growing algorithm requires two parameters to be set: similarity and area threshold. Empirical observations showed that setting similarity values below 50 led to over-segmentation, i.e., creating excessive regions representing details within the same species coverage. Conversely, values above 80 resulted in undersegmentation, producing an insufficient number of segments.

For the area threshold, a range of 50 to 200 was established, because setting values outside this limit also caused the effects of over-segmentation and under-segmentation, without improving segmentation quality itself. However, defining a range does not completely eliminate these effects, it only reduces their occurence. Among the pairs of intervals tested, segmentation with parameters 70/200 (similarity/area) configuration generated the fewest number of segments across the three clippings and was selected for comparison with segmentation using subsampling and smoothing (Figures 2 and 3).

From the tests, it was possible to see that setting lower ranges created too many segments, both for similarity and area threshold, as the requirement to form a region is greater. Thus, more segments were formed in the 0.8 cm and 1 cm subsampled images due to the greater spectral variability response in space. Figures 2 and 3 show a tendency for segments to decrease as the level of detail decreases, which indicates, as expected, that subsampling and smoothing detect less detail in the image. When comparing smoothing and subsampling, smoothing generated approximately 70% fewer segments than subsampling at the first level. At higher levels, the number of segments in both approaches tended to converge.

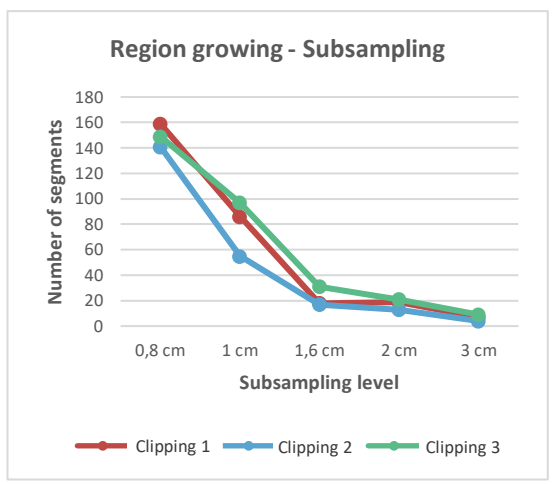


Figure 2. Correlation between subsampling and number of segments created using region growing algorithm.

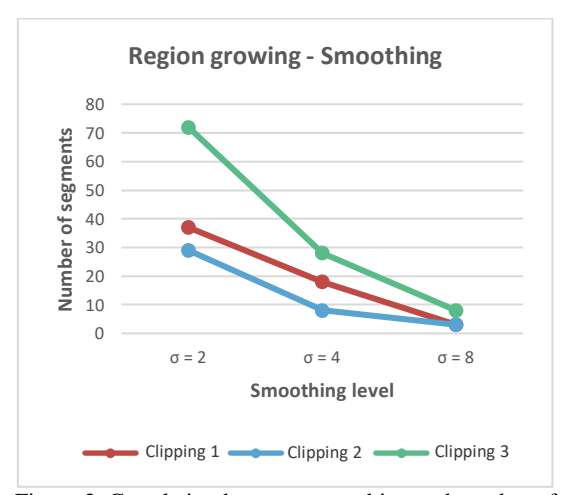


Figure 3. Correlation between smoothing and number of segments created using region growing algorithm.

Since the decrease in spatial resolution creates fewer segments, it is possible to note that region growing algorithm is more sensitive to the level of detail 0.8 cm and 1 cm images than the other levels. In addition, defining the same thresholds for the three clippings generated a different number of segments. This behaviour may be attributed to the unique characteristics of each region (clippings), given that each one has different EAV species, spatially arranged in distinct patterns.

For clipping 1, the 3 cm segmented subsampling effectively separated the two EAV species (Figure 4a), while the 0.8 cm and 1 cm subsamplings led to over-segmentation. A similar pattern occurred for clippings 2 and 3, however, in clipping 2, only the 2 cm subsampling (Figure 4b) produced a consistent segmentation. In clipping 3, none of the segmented subsamplings was able to delineate the species satisfactorily, although the 3 cm subsampling (Figure 4c) came closest.

It can be seen the delineation was flawed in all the clippings, since it included individuals that did not belong to the same species coverage, as well as leaving some of them out due to the entanglement between species. In general, clipping 3 apparently obtained less efficient results in separating EAV, likely due to its complex spatial organization.

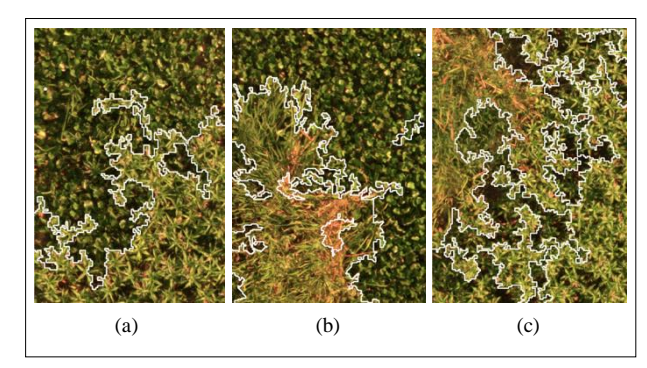


Figure 4. Best delineate segmentations of EAV species in each clipping with region growing algorithm, using the following parameters: Similarity: 70/Area: 200. Subsampling segmentation of (a) 3 cm, (b) 2 cm and (c) 3 cm, respectively. All the clippings in the background are at the original level (0.8 cm).

Smoothing did not generate any groupings that visually corresponded to the separation of EAV species, indicating that the subsampling was more effective in this case. These results suggest that the region growing algorithm is sensitive to illumination changes and significantly influenced by spatial resolution.

3.2 Experiment 2: Superpixel (SLIC)

The SLIC algorithm requires defining the parameter k, number of segments, and optionally adjusting m, compactness, which influences the shape. For compactness, the higher m value, the more regular and rigid the segments will be, and the lower, the more irregular and flexible will appear.

Regarding the k parameter, it is important to note that it represents the approximate number of segments to be generated. Experiments indicated that approximately 50 segments were sufficient to cover a type of EAV in each segment. Higher values led to excessively small segments, especially when considering plant clusters. Based on these findings, the parameters 10/50 (compactness/number of segments) were used to compare the segmentation across subsampling and smoothing techniques.

The superpixel algorithm maintained a consistent number of segments generated in all clippings for all levels of subsampling and smoothing. This contrasts with the region growing algorithm, where segmentation varied with pixel size. Visually, the subsamples segmentation did not show significant differences with the variation in pixel size, compared to region growing algorithm. There are subtle changes in the edges as the pixel size increases, as these contours become more irregular. Despite this, the overall segment shapes remained stable across subsampling levels.

To compare the clippings, Figures 5a-c used the 3 cm subsampling segmentation. Clipping 1 (Figure 5a) created segments containing a set of the same EAV species in the upper left and another species in the lower right of the image, while in the central area exhibited a mixed transition zone. Compared to clipping 1, clippings 2 (Figure 5b) and 3 (Figure 5c) demonstrated a clearer separation of the two species, with less mixing in their transition regions. However, in clipping 3, the spatial organization of EAV resulted in greater spacing between plants, leading to segments containing fewer plants and more shadow areas. For subsampling, it was apparently more challenging to separate the species in clippling 1, as they are

visually more similar when compared to the species in clippings 2 and 3.

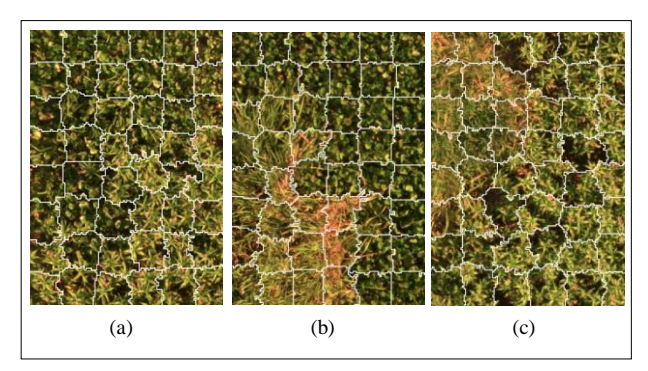


Figure 5. Comparison of 3 cm subsamples in clippings (a) 1, (b) 2 and (c) 3 segmented using superpixel algorithm, with the following parameters: Compactness: 10/Quantity of segments: 50. All the clippings in the background are at the original level (0.8 cm).

The same pattern is also evident in Figures 6a-c on smoothing process, i.e., the segments generated were able to contour and separate the EAV species better in clippings 2 and 3, which occurred in subsampling as well. However, a key distinction in smoothing is that segment edges become softer and shapes more flexible, a characteristic that is accentuated as the degree of smoothing increases, reducing the rigidity of the segments generated in the subsampling.

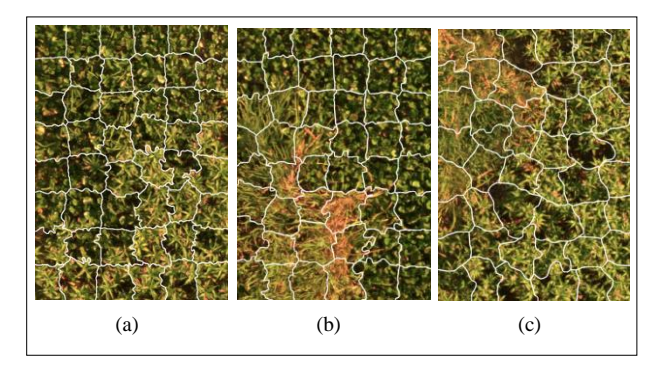


Figure 6. Comparison of clippings (a) 1, (b) 2 and (c) 3 segmented with different smoothing level using superpixel algorithm, with the following parameters: Compactness: 10/Quantity of segments: 50. (a) σ =2; (b) σ =4; (c) σ =8. All the clippings in the background are at the original level (0.8 cm).

Smoothing stood out for superpixel algorithm, as visually the segments are better defined in edgewise. In contrast, subsampling segmentation (Figures 5a-c) retained highly detailed contours, which did not significantly contribute to species separation quality. To demonstrate this behavior, Figure 7 highlights the same segment of clipping 3 in subsampling and smoothing. Notably, the excessive edge details in Figure 7a do not add any relevant information compared to Figure 7b. Thus, smoothing had more consistent results for the superpixel algorithm.

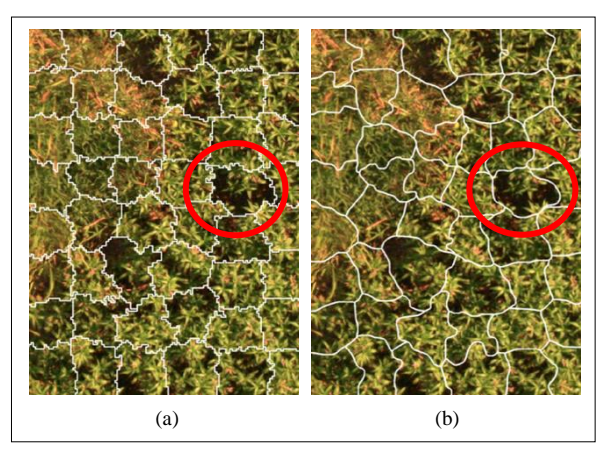


Figure 7. Comparison of the same segment in (a) subsampling (3 cm) and (b) smoothing (σ =8) of clipping 3 for superpixel algorithm, with the following parameters: Compactness: 10/Quantity of segments: 50. All the clippings in the background are at the original level (0.8 cm).

3.3 Experiment 3: Watershed

The Watershed algorithm requires tuning of key parameters, particularly the depth threshold and flood level, which are critical to its performance. Given its inherent tendency for oversegmentation, multiple tests were conducted, yet most results remained highly segmented. However, for comparison purposes, segmentation with parameters 0.01/0.3 (depth threshold/flood level) generated the fewest segments for the three clippings and was used to compare subsampling and smoothing segmentations (Figures 8 and 9).

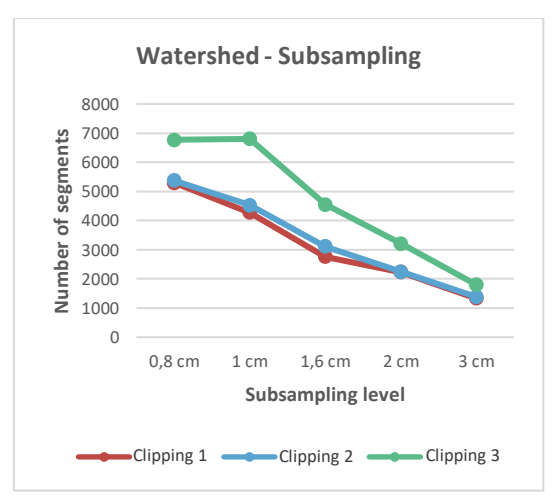


Figure 8. Correlation between subsampling and number of segments created using watershed algorithm.

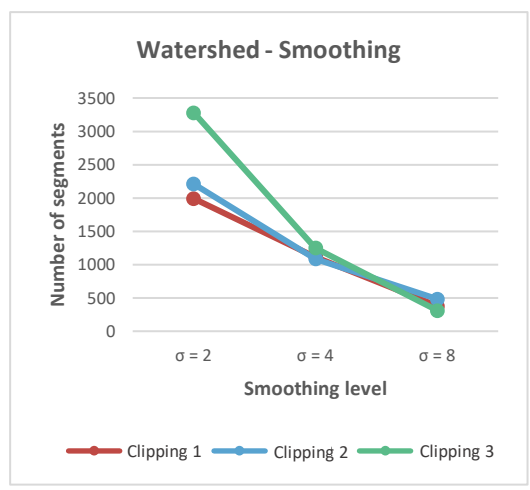


Figure 9. Correlation between smoothing and number of segments created using watershed algorithm.

Watershed behaviour shows similarity to region growing algorithm (Figures 8 and 9), since reducing the level of detail also reduces the number of segments formed. The decrease was approximately 75% from the first to the last level of subsampling, and by 85% from the first to the last level of smoothing. The main difference between the two algorithms is the number of segments generated, since region growing produced 97% and 98% fewer segments at the first level of subsampling and smoothing, respectively, compared to the same levels in the watershed algorithm.

Results for subsampling segmentation were inconsistent, as the algorithm detected excessive detail, causing the effect of oversegmentation. However, subsampling contributes significantly to reducing the number of segments, as does smoothing.

The first two levels of smoothing maintained the effect of oversegmentation (Figures 10a-b). However, the third and highest level (σ =8) generated consistent results, effectively delineating EAV species and forming larger segments, as exemplified by Figure 10c, in clipping 3. Therefore, smoothing stood out compared to subsampling for watershed algorithm, which proved to be more affected by the high level of detail than the region growing algorithm.

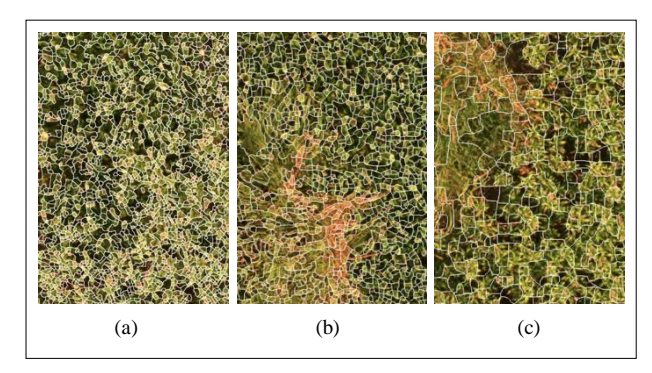


Figure 10. Comparison of clippings (a) 1, (b) 2 and (c) 3 segmented with different smoothing levels using watershed algorithm, with the following parameters: Depth threshold: 0.01/Flood level: 0.3. (a) σ =2; (b) σ =4; (c) σ =8.

3.4 Evaluation of quality segmentation

The quantitative results used to evaluate the quality of the segmentation are presented in Tables 1 to 3, one for each

clipping, comparing the performance of the three segmentation algorithms. For this evaluation, the optimal result for each algorithm was selected: for region growing, the 3 cm subsampling segmentation; for superpixel, the smoothing segmentation with a standard deviation of 4; and for watershed, the smoothing segmentation with a standard deviation of 8.

Entropy - band	Region growing	Superpixel	Watershed
Entropy - R	-2	-0.86675	4.02562
Entropy - G	-2	0.54782	4.45903
Entropy - B	-2	-0.51049	0.55407
Entropy - NIR	-2	-0.45068	4.48288

Table 1. Summarization of entropy for clipping 1 using kurtosis.

Entropy - band	Region growing	Superpixel	Watershed
Entropy - R	7.14877	-0.66345	4.76301
Entropy - G	7.06009	-0.40961	4.29834
Entropy - B	0.85005	-0.92953	-0.39675
Entropy - NIR	7.90339	-1.03827	2.83454

Table 2. Summarization of entropy for clipping 2 using kurtosis.

Entropy - band	Region growing	Superpixel	Watershed
Entropy - R	-1.66601	-0.52187	8.70199
Entropy - G	-1.45591	-0.79042	7.06248
Entropy - B	-1.83116	-0.44127	2.02572
Entropy - NIR	-0.71617	-0.50625	4.94880

Table 3. Summarization of entropy for clipping 3 using kurtosis.

Both region growing and watershed algorithms demonstrated overall kurtosis that indicated different entropy values between segments, resulting in a non-Gaussian distribution. Region growing generated fewer and bigger segments (Figure 4), in contrast, watershed produced more and smaller ones (Figure 10).

These characteristics must have significantly impacted the results of kurtosis once to enclose bigger regions adds greater variability in pixel values, leading to a higher internal entropy, which means less homogeneous segments. Similarly, smaller regions tend to produce highly homogeneous segments with low internal entropy. However, because they often represent distinct scene details, the entropy values vary substantially across segments.

If kurtosis differs substantially from zero, it demonstrates fewer extreme values and more uniform segments in the image context. In all the clippings, kurtosis of four bands for superpixel entropy were closer to zero, which leads to a normal (Gaussian) distribution, meaning a higher internal homogeneity in this study.

4. Conclusions

The results obtained from the three segmentation algorithms showed that region growing and watershed are the most sensitive and affected by high spatial resolution, with over-segmentation being itself one of the limitations of watershed, which produced the largest number of segments, meanwhile superpixel algorithm was less impacted by the same factor and responded better in smoothed clippings. Overall, all of them improved their performance in images pre-processed with subsampling and/or smoothing.

It is important to highlight that the excessive scene detail, due to the high spatial resolution, can interfere on the identification of EAV species successfully, which leads to the importance of simulations and controlled variations in spatial detail using subsampling and smoothing to optimize segmentation.

Additionally, tunning the algorithm parameters is a challenging step, especially for watershed due to its tendency for oversegmentation. Depending on the values set for the input parameters, many scene details have been segmented, such as leaves, shadows, and other minor elements.

On the other hand, the superpixel algorithm generates a fixed number of segments for all clippings, both for subsampled and smoothed versions. This is a feature completely different from the other two, which rely on adaptive parameters to create, at first, an unknown number of segments. This unknown value varies between clippings (regions) and between levels of subsampling and smoothing.

Comparing all the three segmentation algorithms, superpixel generated the most consistent results in delineating the EAV species, considering that it separates them without excessive and unnecessary detail. In addition, the internal homogeneity among segments seems to be better than the other ones, since it was found the near-zero kurtosis of segment entropy in this case.

Furthermore, superpixel is easy to define the parameters which, once defined, can be used for all the clippings (regions), generating satisfying results. In contrast, defining parameters for region growing and watershed algorithms requires many tests before the most suitable parameters are defined, and even what is suitable for one region is often not suitable for another, as these optimal parameters may not be the same for each region, depending on the texture of species present in the scene.

As a result, segmentation plays a critical role in the overall process, as the accuracy of classification depends directly on segmentation quality. The main challenge lies in selecting the most appropriate algorithm and parameter settings to generate meaningful segments aligned with the study purpose.

Acknowledgements

This research was funded by São Paulo Research Foundation FAPESP (2021/06029-7), National Council for Scientific and Technological Development CNPq (Grant: 308747/2021-6).

References

Achanta, R., Shaji, A., Smith, K., Lucchi, A., Fua, P., Süsstrunk, S., 2012. SLIC Superpixels Compared to State-of-the-Art Superpixel Methods. *IEEE Transactions on Pattern Analysis and Machine Intelligence*, 34(11), 2274–2281.

Alagialoglou, L., Manakos, I., Papadopoulou, S., Chadoulis, R.-T., Kita, A., 2023. Mapping Underwater Aquatic Vegetation Using Foundation Models With Air- and Space-Borne Images: The Case of Polyphytos Lake. *Remote Sensing*, 15(16).

Arif, F., Akbar, M., 2005. Resampling Air Borne Sensed Data Using Bilinear Interpolation Algorithm. *International Conference on Mcchatronics*. doi.org/10.1109/icmech.2005.1529228.

Ashworth, W., 2023. Ecological interactions of habitat forming emergent vegetation; With focus on Phragmites australis and Typha sp. Aqua Introductory Research Essay 2023:1. Uppsala: Department of Aquatic Resources.

Benjamin, A.R., Abd-Elrahman, A., GETTYS, L.A., Hochmair, H.H., Thayer, K., 2021. Monitoring the efficacy of crested floatingheart (Nymphoides cristata) management with object-based image analysis of UAS imagery. *Remote Sensing*, 13(4).

Bins, L. S., Fonseca, L.M.G., Erthal, G. J., Mitsuo, F., 1996. Satellite Imagery Segmentation: a region growing approach. *Simpósio Brasileiro de Sensoriamento Remoto*, 677–680.

Blaschke, T., 2010. Object-based image analysis for remote sensing. *ISPRS Journal of Photogrammetry and Remote Sensing*, 65(1), 2–16.

Blaschke, T., Hay, G.J.; Kelly, M., Lang, S., Hofmann, P., Addink, E., Feitosa, R.Q., Van Der Meer, F., Van Der Werff, H., Van Coillie, F., Tiede, D., 2014. Geographic Object-based Image Analysis — Towards a new paradigm. *ISPRS Journal of Photogrammetry and Remote Sensing*, 87, 180–191.

Bolch, E.A., Hestir, E.L., Khanna, S., 2021. Performance and Feasibility of Drone-Mounted Imaging Spectroscopy for Invasive Aquatic Vegetation Detection. *Remote Sensing*, 13(4).

Brooks, C., Grimm, A., Marcarelli, A.M., Marion, N.P., Shuchman, R., Sayers, M., 2022. Classification of Eurasian Watermilfoil (Myriophyllum spicatum) Using Drone-Enabled Multispectral Imagery Analysis. *Remote Sensing*, 14(10).

Du, Q., Kopriva, I., 2008. Automated Target Detection and Discrimination Using Constrained Kurtosis Maximization. IEEE Geoscience and Remote Sensing Letters, 5(1), 38–42.

Espindola, G. M., Camara, G., Reis, I.A., Bins, L.S., Monteiro, A.M., 2006. Parameter selection for region-growing image segmentation algorithms using spatial autocorrelation. *International Journal of Remote Sensing*, 27(14), 3035-3040.

Hyvärinen, A., Oja, E., 2000. Independent component analysis: algorithms and applications. *Neural Networks*, 13, 411–430.

Hossain, M.D., Chen, D., 2019. Segmentation for Object-Based Image Analysis (OBIA): A review of algorithms and challenges from remote sensing perspective. *ISPRS Journal of Photogrammetry and Remote Sensing*, 150, 115–134.

Inglada, J., Christophe, E., 2009. The orfeo toolbox remote sensing image processing software. *International Geoscience and Remote Sensing Symposium*, 733–736. doi.org/10.1109/igarss.2009.5417481.

Kornilov, A. S., Safonov, I.V., 2018. An overview of watershed algorithm implementations in open source libraries. *Journal of Imaging*, 4(10).

Liu, Z.Y.-C., Chamberlin, A.J., Tallam, K., Jones, I.J., Lamore, L.L., Bauer, J., Bresciani, M., Wolfe, C.M., Casagrandi, R., Mari, L., Gatto, M., Diongue, A.K., Toure, L., Rohr, J.R., Riveau, G., Jouanard, N., Wood, C.L., Sokolow, S.H., Mandle, L., Daily, G., Lambin, E.F., De Leo, G.A., 2022. Deep Learning Segmentation of Satellite Imagery Identifies Aquatic Vegetation Associated with Snail Intermediate Hosts of Schistosomiasis in Senegal, Africa, *Remote Sensing*, 14(6).

Long, D., Singh, V.P., 2013. An Entropy-Based Multispectral Image Classification Algorithm. *IEEE Transactions on Geoscience and Remote Sensing*, 51(12), 5525–5238.

- Mqingwana, P., Shoko, C., Gxokwe, S., Dube, T., 2024. Monitoring and assessing the effectiveness of the biological control implemented to address the invasion of water hyacinth (Eichhornia crassipes) in Hartbeespoort Dam, South Africa. *Remote Sensing Applications: Society and Environment*, 36.
- Roy, D.P., Dikshit, O., 1994. Investigation of Image Resampling Effects upon The Textural Information Content of a High Spatial Resolution Remotely Sensed Image. *International Journal of Remote Sensing*, 15(5), 1123-1130.
- Singh, G., Reynolds, C., Byrne, M., Rosman, B.A., 2020. Remote Sensing Method to MonitorWater, Aquatic Vegetation, and Invasive Water Hyacinth at National Extents. *Remote Sensing*, 12
- Sun, Y., He, G., 2008. Segmentation of High-resolution Remote Sensing Image Based on Marker-based Watershed Algorithm. *Fifth International Conference on Fuzzy Systems and Knowledge Discovery*, 271–276. doi.org/10.1109/fskd.2008.249.
- Szabó, L., Bertalan, L., Szabó, G., Grigorszky, I., Somlyai, I., Dévai, G., Nagy, S.A., Holb, I.J., Szabó, S., 2024. Aquatic vegetation mapping with UAS-cameras considering phenotypes. *Ecological Indicators*, 81.
- Van Der Walt, S., Schönberger, J.L., Nunez-Iglesias, J., Boulogne, F., Warner, J.D., Yager, N., Gouillart, E., Yu, T., 2014. Scikit-image: Image processing in python. *PeerJ*.
- Virtanen, P., Gommers, R., Oliphant, T.E., 2020. SciPy 1.0: fundamental algorithms for scientific computing in Python. *Nature Methods*, 17, 261–272.
- Wang, Y., Gong, Z., Zhou, H., 2023. Long-term monitoring and phenological analysis of submerged aquatic vegetation in a shallow lake using time-series imagery. *Ecological Indicators*, 154
- Yu, Z., Xie, T., Zhu, Q., Dai, P., Mao, X., Ren, N., Zhao, X., Guo, X., 2024. Aquatic plants detection in crab ponds using UAV hyperspectral imagery combined with transformer-based semantic segmentation model. *Computers and Electronics in Agriculture*, 227.
- Zhou, R., Yang, C., Li, E., Cai, X., Yang, J., Xia, Y., 2021. Object-based wetland vegetation classification using multifeature selection of unoccupied aerial vehicle RGB imagery. *Remote Sensing*, 13(23).